

Redox Active Polymer as a pH Actuator on a Re-Sealable Microfluidic Platform

Divya Balakrishnan^{1,2}, Mathieu Gerard¹, Doriane Del Frari¹, Stephanie Girod¹, Wouter Olthuis² and César Pascual-García^{1*}

¹Material Research and Technology Department (MRT), Luxembourg Institute of Science and Technology (LIST), 41 Rue du Brill, L-4422 Belvaux, Luxembourg, Europe
²MESA+, University of Twente, Drienerlolaan 5, 7522 NB Enschede, The Netherlands

Abstract

The electrochemical control of molecular concentrations in liquids is quite challenging because of the small ratio of interacting sites between the electrode surface and the number of molecules in the volume. Here we review our recent works aiming the control of proton concentration combining redox self-assembled monolayers with a modified platform. We used Aminothiophenol, to obtain coatings with quasi-reversible redox states able to exchange protons with the electrolyte at low voltages using different polymerization methods. We studied their charge exchange during different cycles, which would provide us the possibility to use different cycles of reactions controlled by acidity. We achieved the control of proton concentration over the liquid with an efficient design of the microfluidic device to control the diffusion of protons avoiding the reduction of hydrogen at the counter electrode and providing long lasting stability to carry control of chemical reactions during several tenths of minutes. The experiments were carried out in aqueous environment using a pH fluorescence marker to track the pH that allowed us to monitor the proton concentration down to pH 5, where the fluorescence molecule lost its sensitivity, while calculations indicate that the pH can be below 1.

Keywords: Microfluidic platform; Electrochemical cell; Miniaturization; pH control

Introduction

Redox active self-assembled monolayers (SAMs) are materials capable of exchanging electrons and ions between electrodes and electrolytes that can facilitate the design of devices like sensors, batteries, or chemical switches [1]. In these devices the changes in the liquid make the chemical modifications on the electrodes to provide them some functionality. In other cases, the electrodes can be conceived as actuators to change the chemical environment [2]. The acidity is one of the main factors of the chemical environment facilitating the control of reactions like the synthesis of polymers [3], the activation of enzymes [4] or physical properties like the swelling of polymer hydrogels [5]. The efficiency to control other chemical processes through the electrochemical generated acid will depend on the proton concentration range achievable, the number of reversible cycles that can be repeated and that the applied voltages to generate or uptake protons do not interfere with the other chemical reactions that want to be controlled. Nevertheless, the control of the proton concentration from electrodes is quite challenging mainly because it is proportional to the surface to volume ratio of the electrodes, which is unfavorable in normal conditions leading to very small changes of acidity.

Different methods to achieve control of the acidity have been explored in literature. The simplest one in water is electrolysis [6], which separates the water molecules into H^+ and OH^- ions at voltages over 1.23 V (against normal H^+ reference electrode). Though this method is easy to implement, the disadvantage is that it is an irreversible reaction and that the high potentials could trigger some other reactions with the chemicals in solution. To reduce the energy of the reactions and achieve some quasireversibility the electrode surfaces can be coated with redox active conducting polymers like PEDOT or polypyrrole [7,8]. The disadvantage is that polymers coatings tend to degrade with repeating reactions through excess of crosslinking showing poor reversibility. The impact of the redox reactions to change the pH can also be very low due to the unfavorable surface to volume ratio. An alternative approach can be using redox active molecules like hydroquinone and benzoquinone

in the electrolyte that exchange protons [9]. The molecules in contact with the electrode can be oxidized or reduced to change the pH. Using this approach the pH change close to the electrodes was used to control different chemical reactions but the protons diffuse rapidly, so that the pH control was not uniform over a large volume. Also, though the working potentials were lower because it avoided the potential drop across several monomer bonds, the problems of electrode degradation and low pH changes can also be a problem in this case. To increase the surface area and the impact of the redox reactions, Willner and his group reported the electrochemical change of pH in a confined volume using a three dimensional layer of Au nanoparticle composites. The composites were electrochemically deposited by crosslinking the thiol functionalized Au nanoparticles with an electrode surface functionalized with SAMs of Aminothiophenol [10]. The system showed reversible reactions for several cycles with a pH range of ± 1 pH units. A different approach was adopted by Wang et al. to achieve large pH ranges. Instead of changing the electrodes they constructed a device separated by an interfacial Pd thin film that allowed reduction in one side and oxidation in the other, obtaining opposite changes of pH in each of the cells [11]. This device achieved a large useful pH range between 5 and 11.

The advantage of SAMs to change the acidity is that they can be easily used to obtain highly ordered layers with low redox voltages that can exchange protons in aqueous or organic environments. Aminothiophenol (ATP) is an organic molecule able to form SAMs in noble metals thanks to the affinity of its mercapto group and the

*Corresponding author: Cesar Pascual-García, Material Research and Technology Department (MRT), Luxembourg Institute of Science and Technology (LIST), 41 Rue du Brill, L-4422 Belvaux, Luxembourg, Europe, Tel: +352 275 888 583; E-mail: cesar.pascual@list.lu

Received May 21, 2018; Accepted May 29, 2018; Published June 09, 2018

Citation: Balakrishnan D, Gerard M, Frari DD, Girod S, Olthuis W, et al. (2018) Redox Active Polymer as a pH Actuator on a Re-Sealable Microfluidic Platform. J Material Sci Eng 7: 456. doi: [10.4172/2169-0022.1000456](https://doi.org/10.4172/2169-0022.1000456)

Copyright: © 2018 Balakrishnan D, et al. This is an open-access article distributed under the terms of the Creative Commons Attribution License, which permits unrestricted use, distribution, and reproduction in any medium, provided the original author and source are credited.

interactions among the benzene rings [12,13]. The dissociation constant (pK_a) of the amino-group and its interaction with protons has been used to fabricate plasmonic pH sensors associating the molecule to metal nanoparticles to enhance the vibronic signatures that reveal the protonation state of the molecule [14,15]. ATP can also provide reversible redox active reactions in its polymerized state at low voltages to exchange protons. Though in normal SAMs electrodes the surface volume is very unfavorable within the correct device it can be used to control the pH.

In this paper we review our latest works studying pH modifications using ATP. We studied different methods of polymerization of ATP including the well-studied electrochemical polymerization and less common ones like photo-polymerization and plasma polymerization attending to the charge transfer, which is the main factor from the SAM's that can influence the pH change. Then we combined the most efficient method with a device that addresses the challenge miniaturizing the pH control through the design of a microfluidic platform. The difference with previous works is that in our case we took care that the device could be compatible with miniaturization and the use of small volumes. In this paper we include details of the model and calculations to put an emphasis on the rules we used to obtain a design of a platform that allowed the use of SAMs to change the pH in more than 6 units in reduced volumes avoiding the degradation of the electrodes. We provide additional details of the fabrication process that we followed to produce chips that are integrated on the platform. Finally, we provide the conclusions and perspectives of such device combined with the improvements of new polymerization methods.

Materials and Methods

Study of the redox coatings

Sample preparation to study redox reactions of ATP: Silicon with 50nm thermal grown oxide layer was cleaved to obtain $2 \times 1 \text{ cm}^2$ samples that were evaporated with Au 30 nm with an adhesion layer of Ti 5 nm using an e-beam evaporator. We achieved low roughness ($<2 \text{ nm}$) using an evaporation rate of 0.9 \AA/s at a pressure of 10^{-9} mbar . Substrates were then cleaned under a UV ozone lamp for 30 minutes. 0.5 mM concentration of 4 Aminothiophenol solution in 30 ml of absolute was prepared in a beaker. After the completion of UV ozone cleaning, the samples were placed on the thiol solution beaker and covered with aluminum foil. The beaker was placed under a fumehood for overnight functionalization.

Methods of polymerization: Three different methods of polymerization of ATP were performed, Electropolymerization, Photopolymerization and Plasmopolymerization. Electropolymerization was carried out by cyclic voltammetry using a Princeton applied research Versastat MC potentiostat. The experimental set-up used was a three electrode electrochemical cell with the ATP functionalized Au as working electrode, platinum wire as counter electrode and a calomel reference electrode. Everything was mounted inside a Faraday cage with the beaker with the electrolyte mounted on top of a stage to adjust the height of the exposed working electrode that was fixed to a stand in the Faraday cage. The electrolyte used had 1 M concentration of phosphate buffer solution purged with N_2 for five minutes before performing the experiment. The CV cycles were programmed in the potentiostat with a voltage range between -0.2 to 0.7 V , at 100 mV/s for 5 cycles.

For photopolymerization or ultra violet polymerization (UV), the substrate functionalized with ATP was placed in a beaker containing 1 M concentration of phosphate buffer solution. The beaker was placed

under a UltraViolet lamp of power 0.9 mW/cm^2 and wavelength of 365 nm for 30 minutes. Finally, for plasma polymerization, the ATP functionalized substrate was placed on a plane-to-plane direct dielectric barrier discharge plasma generator at atmospheric pressure. Argon plasma with a voltage of $0.4\text{-}0.6 \text{ kV}$, frequency 10 kHz and a gas flow of 20 L/min for two runs is exposed on the substrate.

Electrochemical performance of the polymerized layers: The charge transfer for each polymerization method was calculated from CV measurements in the same setup and experimental conditions described for the electro polymerization of ATP. The experiments were recorded for the voltage range of -0.2 to 0.7 V at 100 mV/s scan rate. The reversibility of the redox reactions were tested by repeating the cycles for up to 50 times.

Implementation in a microfluidic platform

Fabrication of the electrochemical cell chip for miniaturized control of pH: The electrochemical cell chip was fabricated on a $3 \times 3 \text{ cm}^2$ Si Substrate with 50 nm oxide layer using optical lithography (Figure 1). The cell chip consisted of a platinized working electrode (WE) which was connected to a platinized counter electrode (CE) and Au pseudo reference electrode (RE) each by diffusion barriers (Figure 1a and 1b). The dimensions of the cell are area of WE $A_{we} \sim 0.05 \text{ dm}^2$, total area of the cell $A_{cell} \sim 0.1 \text{ dm}^2$, length L_{ch} and width W_{ch} of the diffusion barrier $\sim 2.6 \text{ cm}$ and $\sim 100 \text{ }\mu\text{m}$ respectively, the height of the cell $h=3.5\text{ }\mu\text{m}$ and the volume of the cell $V_{cell} \sim 120 \text{ nL}$. The complete fabrication process (Figure 1c-e) we used goes as follows; optical lithography was performed using a maskless laser writer MLA 150 from Heidelberg instruments. Two designs were made using Klayout CAD design program [16]. The first design (M1) included the design of the electrodes with the contact pads. For the M1 design, the substrate was spincoated with LOR 3A (300nm) and S1813 (1.3 μm) photoresist. Using the laser writer the substrates were exposed with the design M1 with an exposure dose of 120 mJ/cm^2 . Then the samples were developed in MF319 solution for 50 seconds and blow dried with N_2 .

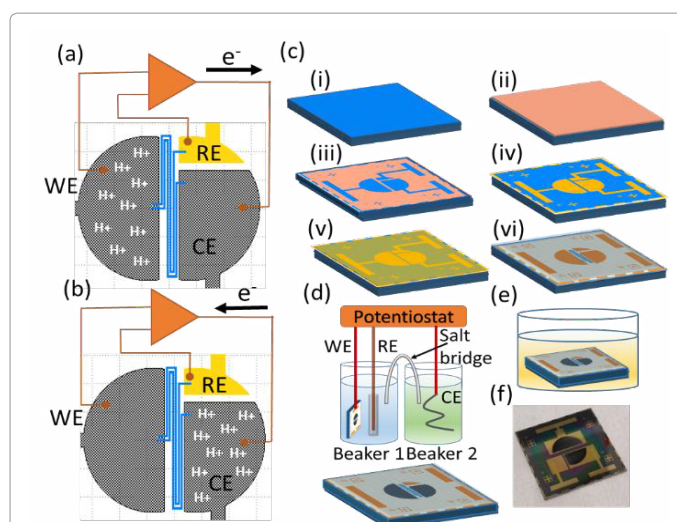


Figure 1: Schematic representation of the electrochemical cell (a) for the oxidation reaction increasing proton concentration in the WE and (b) for the reduction reaction to recover the more basic conditions. (c) Fabrication of the electrochemical cell: a $3 \times 3 \text{ cm}^2$ SiO₂/Si substrate (i) is spin coated with optical resist (ii) the first layer of optical lithography (Layer M1) is defined with laser lithography (iii) and Ti/Au electrodes are e-beam evaporated (iv), second layer of SU8 optical resist is spin coated (v) and optical lithographed (layer M2) (vi) (d), Representation of the Latinization of WE and CE (e) representation of the ATP functionalization. (f) Picture of the fabricated electrochemical chip.

The photolithographed samples were placed on an e-beam evaporator and 5 nm Titanium and 50 nm of Gold were evaporated. The Lift-off process was carried out in a beaker containing 50 ml of acetone. After 15-20 minutes the photo resist S-1813 dissolves leaving the patterned electrodes. The sample was rinsed with distilled water and blow dried with nitrogen. The evaporated sample was again spin coated with SU8 2005 epoxy resist at 5500 rpm and baked at 95°C for 1 mins to obtain a uniform layer of 3.5 μm thickness. The second design (M2) had the definition of the cell volumes with the diffusion barriers along with the opening for contact pads and electrodes. The substrate was then loaded into the laser writer for the second lithography of design M2 with an exposure dose of 1000mJ/cm². The sample was then baked before developing at 95° for 3 minutes and then inserted into MICRO-CHEM SU8 developer solution for 1 minute and dried with nitrogen.

Platinisation of electrodes: The experimental set-up (Figure 1d) was as follows: beaker 1 contained 40 mM of chloroplatinic acid and 100 μM lead acetate solution in distilled water, beaker 2 contained 1 M of phosphate buffer solution. A salt bridge was made with a filter paper strip that was immersed in potassium chloride solution, after removing the excess of electrolyte it was placed between the two beakers. The salt bridge was immersed in both liquids of the beakers. Using a clamp, the working electrode contact pad of the sample was connected to the potentiostat. The sample was immersed in beaker 1 covering the electrode to be platinized. We used a Ag/AgCl reference electrode immersed in beaker 1. The Pt counter electrode was immersed in beaker 2. A cyclic voltammogram experiment was created using the potentiostat between the voltage range -0.2 V to 0.6 V at a scan rate of 100 mV/s for 4 cycles. After the completion of the 4 cycles, the sample was removed from the beaker and washed with distilled water, ethanol and blow dried with nitrogen. The counter electrode was also platinized following the same procedure. Then sample was cleaned with ethanol, water and placed under UV lamp for 30minutes. Finally the sample (Figure 1c) was functionalized with ATP by following the same procedure as explained in previous section.

Description of the microfluidic platform: The μ -fluidic platform to hold the chip consisted of two parts with top and the bottom frames (in yellow and grey respectively in Figure 2a-2e. The top frame included

a glass window that provided optical access, the μ -fluidic inlet and outlet for the flow of liquids and the electrical contacts. The contacts to the chip were made through springs and they were connected to a switching box allowing the electrodes to be grounded or connected to the potentiostat. The bottom frame included the sample stage with a pneumatic actuator (in blue) using compressed air to lift the chip after the liquid was inserted in the channel, leaving in these way the cells connected only through the electrolyte in the diffusion barriers. The two parts were sealed with an elastic O-ring (Figure 2c) and closed by screws. The chip on the stage (in blue) could be moved up (cell closed) or down (cell open) by opening the valve of the compressed air (V1). In open position, the O-ring pushed down the chip allowing a 60 μm gap between the chip and the glass window on the top frame. This position will allow the filling and exchange of liquids in the cell. In closed position the chip was pushed up in contact with the glass window on the top frame and the cells are isolated from μ -fluidic channel and are only connected through diffusion barriers. A syringe with the electrolyte was connected to the μ -fluidic inlet tube (V2) and an empty syringe is connected the μ -fluidic outlet tube (V3). A vacuum pump was connected to the other inlet of T-valve V3, and to ensure the complete filling vacuum was done before inserting the electrolyte.

Optical set-up: In Figure 2f, the optical set-up was built above the platform for optical inspection through the glass window on the top frame. pH change inside the electrochemical cell was detected using fluorescence dye carboxy semi-naphthorhodafluors (carboxy SNARFs). These molecules are excited using a 565 nm diode source through a dichoric mirror CROMA-49017 with an excitation window between 540 nm and 580 nm and with a low band pass filter at 590nm for collection. The excited area was limited by the focusing/collective objective to a field of view smaller than the WE. In order to increase the fluorescence signal all the light collected by the objective was sent to a wide range spectrometer FLAME-S-VIS-NIR. SNARF fluorescence has two peaks at 590 and 650 nm. The peak at 590 nm is dominant for acidic pH and 650 nm peak in dominant for neutral pH, and the ratio between the two peaks can be used to track the pH in the range from 8 to 5 [17]. The peak at 590 nm is much weaker than the one at 650 nm, and the signal at high proton concentrations became very weak. For this reason we used the ratio of the two peaks to assess the initial pH

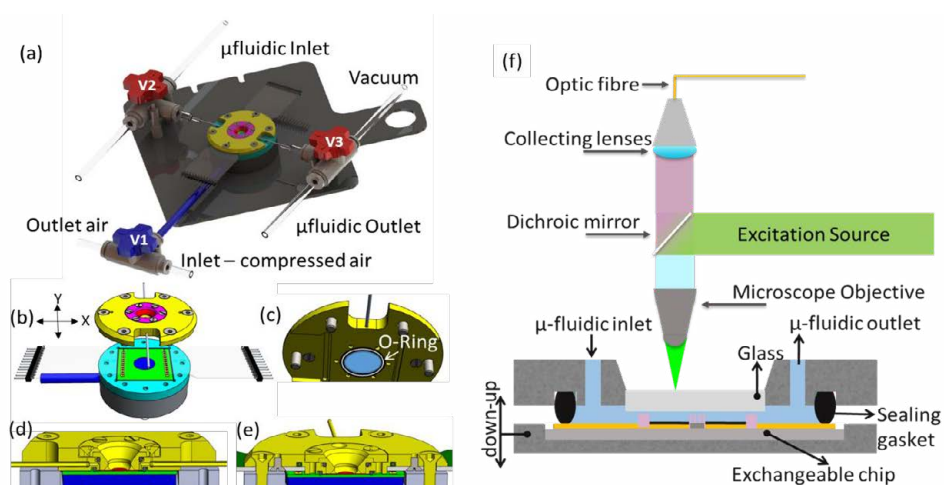


Figure 2: (a) Pictorial representation of the set-up of the microfluidic platform with valves for fluidic transport and pneumatic actuation, (b) opened platform showing the top frame in yellow, bottom frame in grey holding the chip in green. (c) The underlying view of the top frame containing the glass and the O-ring. (d) Cross-section view of the chip mounted on the platform along X axis showing the inlet and outlet for microfluidic transport. (e) The same along Y-axis showing the springs of the electrical contacts on the top to connect the chip. (f) Schematic representation of the microfluidic platform with the optical setup.

and we followed the total pH using the 565 nm excitation. More details about the calibration of SNARF are reported in the supplementary information. The spectra were integrated for 10 seconds.

Electropolymerization and pH control on the platform: The electropolymerisation was performed with the cell in its opened position. For these experiments and all the others in the platform we used a Solartron Modulab XM Pstat 1mS/s potentiostat using three electrode configuration. A cyclic voltammogram was programmed in the potentiostat between of -0.9 V to 0.9 V using a scan rate of 50 mV/s for 4 cycles.

Before the pH control experiments, the cell was flushed exchanging the electrolyte between the two syringes in the circuit. The cell was then closed using the valve V1, leaving the WE communicate to the RE and CE only through diffusion barriers. A cyclic voltammetry experiment is pre-programmed in the potentiostat for a voltage range of 0.75 V to -0.75 V at a scan rate of 50 mV/s. The fluorescence acquisition was started with before the voltage scan, focusing on the signal from the WE.

Results

Polymerization and reversibility of redox reactions of ATP

Figure 3a-3i shows the structural representation of the self-assembled ATP adsorbed on Au, which can be polymerized in different ways (Figure 3ii-3iv) depending on the polymerization method. We discussed the different possibilities of polymerization in our previous article [18]. All the three methods provided reversible proton exchange reactions were 2 protons and 2 electrons are exchanged from the molecule to the electrolyte. Figure 2b shows representative cyclic voltammograms (CV) of the polymerized samples electropolymerized in black, UV polymerized in red and plasma polymerized in blue. Redox active behavior was observed in all the cases with an oxidation and reduction potential around ~0.2 V and ~0 V respectively. The total

charge exchange (Q) of these peaks could be calculated from the area withstanding below the redox peaks:

$$Q = \frac{1}{v} \int_{V_1}^{V_2} I \cdot dV - (V_2 - V_1) \left\{ I_1 + \frac{1}{2} (I_2 - I_1) \right\} \quad (1)$$

Figure 3a shows a representative example of the limits of the peak chosen to make this calculation.

To study the reversibility of redox reactions of the different polymerization types we repeated 50 CV cycles. In Figure 3c the charge transfer for the oxidation and reduction peaks are plotted against the number of cycles. We observed that while electropolymerization initially showed a higher charge transfer respect to the other methods and afterwards it degraded to approximately the same value of the other polymerization methods. In the other hand, the charge transfer of the UV and plasma polymerization was nearly constant and shows less degradation with successive cycles. The advantage of electropolymerization is a higher charge transfer at the beginning, however, UV or plasma polymerizations are more suitable for delivering large batches of samples. If the application intends many cycles, they do not have much difference of charge transfer after 50 cycles. More details of the characterization and performance of the polymerized layers can be found in our previous work [18].

Modelling the pH actuation in the cell

To model the pH changes in the cell shown in Figure 1a due to proton exchange reactions like the ones described above, we assume that the charge transfer from the electropolymerized layers corresponds only to proton exchange reactions and that the initial proton concentration in the WE electrode is negligible, which can occur in water if the total change of pH is several units. We also assume that the protons are confined (and thus they cannot be reduced at the CE), which occurs if the diffusion time across the barriers is much longer than the CV cycles.

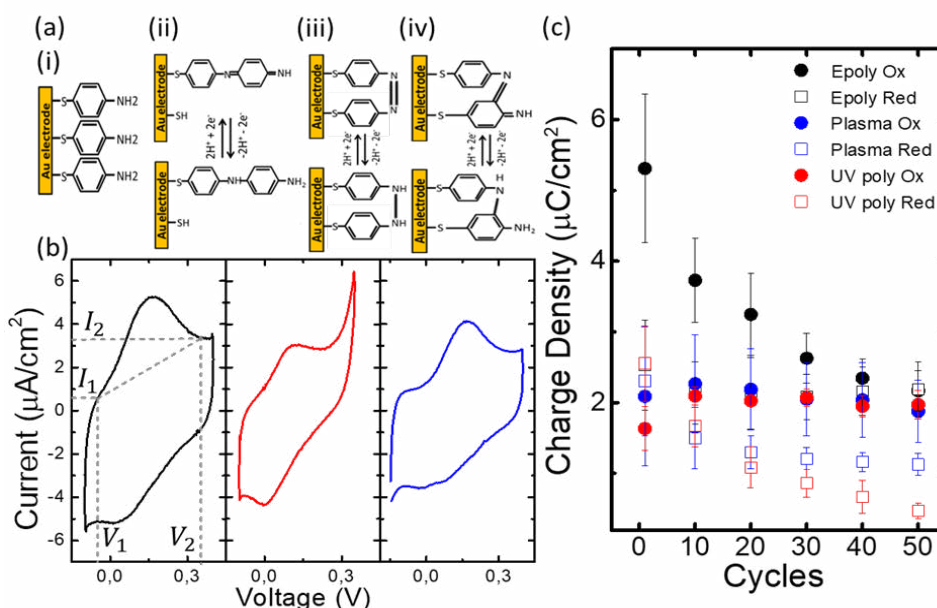


Figure 3: (a) Structural representation of (i) Aminothiophenol, (ii) electropolymerized, (iii-iv) optical and plasma polymerized SAMs on Au electrodes. (b) Cyclic voltammograms of the polymerized layers where black, red and blue correspond to electrochemical, optical and plasma methods respectively. (c) Charge transfer for oxidation and reduction reactions of ATP for different polymerization methods is plotted against the number of cycles. (Figure adapted from our previous publication in 18).

The cell in Figure 1a is a 3 electrode electrochemical cell with WE, CE and RE separated by diffusion barriers. To provide an example of how the cell can control the pH we will assume that the electrode materials are the ATP coated flat electrodes with same surface coverage as described above. With an applied voltage, the ATP molecules exchange protons with the solution thereby changing the pH from higher (neutral) (Figure 1b) to lower (acidic) (Figure 1a) and vice versa. The diffusion barrier separates the electrodes into different cells connected by a narrow long channel. In order to avoid diffusion of protons, the length of the barrier was designed extensively longer than the width and height of the barrier and this increase the diffusion time of protons. A barrier length of 2.6 cm is chosen and for this length, the diffusion time (t) needed for each proton to reach the CE was calculated using the proton diffusion coefficient $D=9E10^{-5} \text{ cm}^2/\text{s}$ [19].

$$t = \frac{(l_{\text{ch}})^2}{D} = 130 \text{ minutes} \quad (2)$$

We assume at this point that the total charge involved in the redox process is the one derived from the peak where the limits are indicated in the cyclic voltammogram data of the electropolymerization process in Figure 3b and the surface coverage (S) of the ATP molecules is calculated.

$$S = \frac{Q}{A \cdot F} = \frac{4.671 \times 10^{-6} \text{ Ccm}^{-2}}{96485.33 \text{ Cmol}^{-1}} = 4.84 \times 10^{-11} \text{ mol/cm}^2 \quad (3)$$

where the area chosen was the footprint of the WE of the chips in in Figure 1 and F is the Faraday constant.

Another factor that contributes to the loss of protons is migration across the barrier. High concentration of electrolyte (1M KCL) is used to avoid migration and to decrease the over potential across the barrier.

After a complete CV oxidation, the maximum number of protons (N) that can be in solution are the ones corresponding to the surface area of the electrodes. The minimum possible pH will correspond to

the distributions of these protons in the volume of the WE, which can be calculated as follows:

$$\text{pH} = -\log \left[\frac{N}{V_{\text{we}}} \right] = -\log \left[\frac{S \cdot A_{\text{we}}}{h \cdot A_{\text{we}}} \right] = -\log \left[\frac{S}{h} \right] = -\log \left[\frac{4.84 \times 10^{-11} \text{ molcm}^{-2}}{3.5 \mu\text{m}} \right] = 3.9 \quad (4)$$

where A_{we} and V_{we} corresponds to Area and volume of the working electrode respectively and h is the height of the cell. Again for an estimation of the possible pH with our fabrication parameters we have used the dimensions from the chips in Figure 1 and the data from the electropolymerization in Figure 3b.

In order to increase the impact of the electrodes in the pH we increased the surface area by platinizing, leading to an effective surface charge normalized to the footprint, which was much higher.

pH control experiments on the re-sealable platform

The reversible states in our chip were achieved through an electropolymerization in the platform. Figure 4 shows the cyclic voltammogram of the electropolymerization process on the chip as a function of voltage (a) and time (b), with reversible oxidation and reduction peaks around 0.2 V vs the cell gold pseudo reference electrode. During the first rise of current (in black) an increase of the slope after 0.6 V can be observed that corresponds to the polymerization. This process is similar to what we observed in our previous work [18], although some changes were observed in the value of the voltages because of the pseudoreference electrode and the materials used in the counter-electrode. For each cycle the current density increases. We attribute this effect to additional polymerization of ATP to form redox active molecules, which were not able to polymerize in the first oxidation.

The pH changes which were simultaneously monitored by measuring the fluorescence at the WE through the SNARF fluorescence marker dissolved in the electrolyte. We used SNARF molecule to monitor the pH behavior (details of the SNARF fluorescence behavior and calibration is included in supporting information). Figure 4c shows

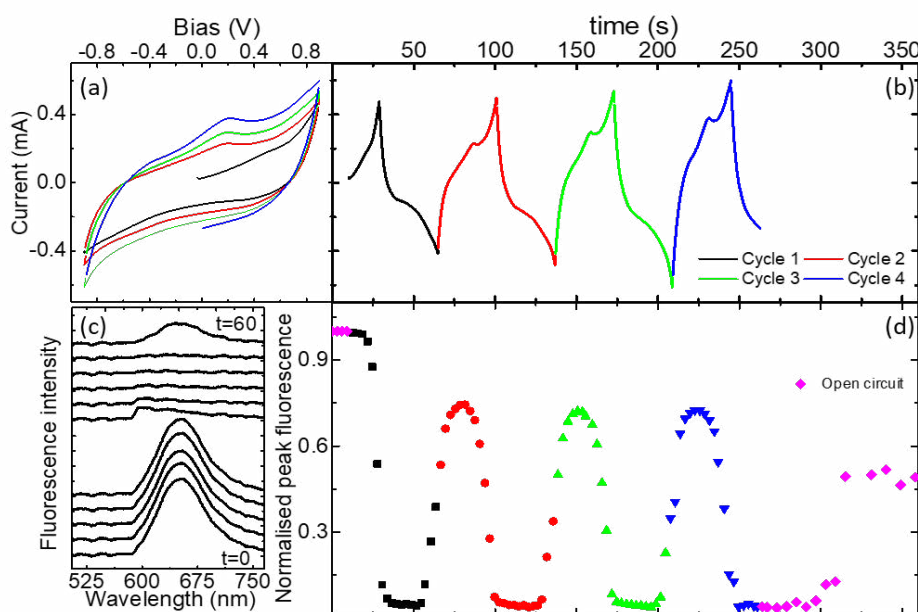


Figure 4: CV of ATP corresponding to the electropolymerization on the chip as a function of voltage (a) and time (b). (c) Sequence of SNARF fluorescence spectra during the first cycle of polymerization. (d) Peak intensity of the fluorescence normalized to its maximum value at neutral pH as a function of time during the polymerization cycles.

fluorescence during the first rise in black. SNARF has two peaks at 590 and 655 nm which are dominant at acidic and basic pH respectively, however at acidic pH's the overall intensity is much weaker. For this reason we could use the relative intensity of the peaks to verify the initial neutral pH, and then, followed the pH with the intensity of the 655 nm peak. In Figure 4c the first four spectra from the bottom correspond to the initial state with neutral pH. In the next spectrum, the 590 peak is more dominant showing that the pH had decreased. This corresponds to the polymerization and the subsequent oxidation. When the acidity increases the spectra are quenched, indicating that the fluorescence marker is beyond its acidity range (~ pH 5). The spectra is recovered after 60s, in the last spectrum shown after the reduction, which recovers protons into the coating.

In Figure 4d the intensity of the 655 nm is shown versus time for all the cycles. This switch of pH from higher to lower is repeated with successive cycles. The changes in acidity proved that the redox reactions involved the exchange of protons. These pH changes were observed because the cell was still only 60 μm , but the pH increased with time, as it can be observed by the raise of the fluorescence occurring after the last cycle in blue.

After the polymerization, the cell was closed to observe the pH changes with confined protons. Figure 5 shows the CV of 8 cycles representing the proton exchange reactions of ATP in a closed cell. (a) The applied voltage and (b) the measured current with respect to time are plotted. The corresponding SNARF fluorescence spectra is extracted and plotted against time in (c). For each cycle the fluorescence intensity

shifts from maximum to minimum and this process is repeated for successive cycles showing reversible pH changes. Using the pH calibration curve of the SNARF fluorescence marker [SI] the maximum and minimum intensity corresponds to pH 7.2 and 5 respectively. The minimum pH achieved is beyond the detection limit of the SNARF fluorescence marker. Using the CV plot the lowest pH (using eqn. (1)) was calculated as 0.9. A more detailed information about the SNARF fluorescence marker and CV experiments were reported in our previous publication [20].

In summary, we have presented a molecule, ATP that traditionally was used for sensors thanks to its ability to exchange protons, but that in a smart microfluidic device, we have been able to use it to change the pH in nanoliter volumes. We have reviewed the routes to obtain reversible redox states by polymerizations, and the efficiency of the redox active reactions achieved. A miniaturized electrochemical cell of few 100 nL was modelled to control the pH. The detailed steps involved in the fabrication process and the design of the platform are explained. We have presented how to control critical parameters involved in the design of the cell like diffusion time of protons through the barrier, dimensions of the cell and the estimation of minimum pH that could be achieved with flat electrodes. We have demonstrated a setup involving our platform to monitor the pH changes in these volumes, in the electropolymerization and in the pH control experiments.

The cell that we have presented is compatible with miniaturization. Eqn. (4) shows that the minimum pH does not depend on the area of the electrodes, thus different designs could be implemented depending only on the effective surface coverage of ATP and the height of the cell in its closed position. This opens the way to new designs that could include further nanostructuring of the electrodes, other than platinisation to control the effective surface area in a rational way. The single channel architecture of our cell is also compatible with the inclusion of several cells, which would allow multiplexing of pH control in a single device. For these novel implementations, the presented methods of polymerization provide flexibility for mass production outside the chamber, and post modification of the electrodes for example ion permeable layers.

In conclusion, we believe that our platform can open the way to the control of chemical reactions through the systematic control of proton concentration, allowing miniaturization and multiplexing.

Acknowledgement

This investigation was financed by the FNR ATTRACT project 5718158 NANOpH.

References

- Eckermann AL, Feld DJ, Shaw JA, Meade TJ (2010) Electrochemistry of redox-active self-assembled monolayers. *Coord Chem Rev* 254: 1769-1802.
- Penner RM (2010) Electrochemistry: Protons on tap. *Nat Chem* 2: 251-252.
- Gao X, Yu P, LeProust E, Sonigo L, Pellois JP, et al. (1998) Oligonucleotide synthesis using solution photogenerated acids. *J Am Chem Soc* 120: 12698-12699.
- Cleland WW (1982) The use of pH studies to determine chemical mechanisms of enzyme catalyzed reactions. *Methods in Enzymology* 87: 390-405.
- Chunl BS, Jhona MS, Leeb HB, Yukb SH (1998) pH/temperature dependent phase transition of an interpenetrating polymer network: anomalous swelling behavior above lower critical solution temperature. *Eur Polym J* 34: 1675-1681.
- Morimoto K, Toya M, Fukuda J, Suzuki H (2008) Automatic Electrochemical Micro-pH-Stat for Biomicrosystems. *Anal Chem* 80: 905-914.
- Shinohara H, Kojima J, Aizawa M (1989) Electrically controlled ion transfer and

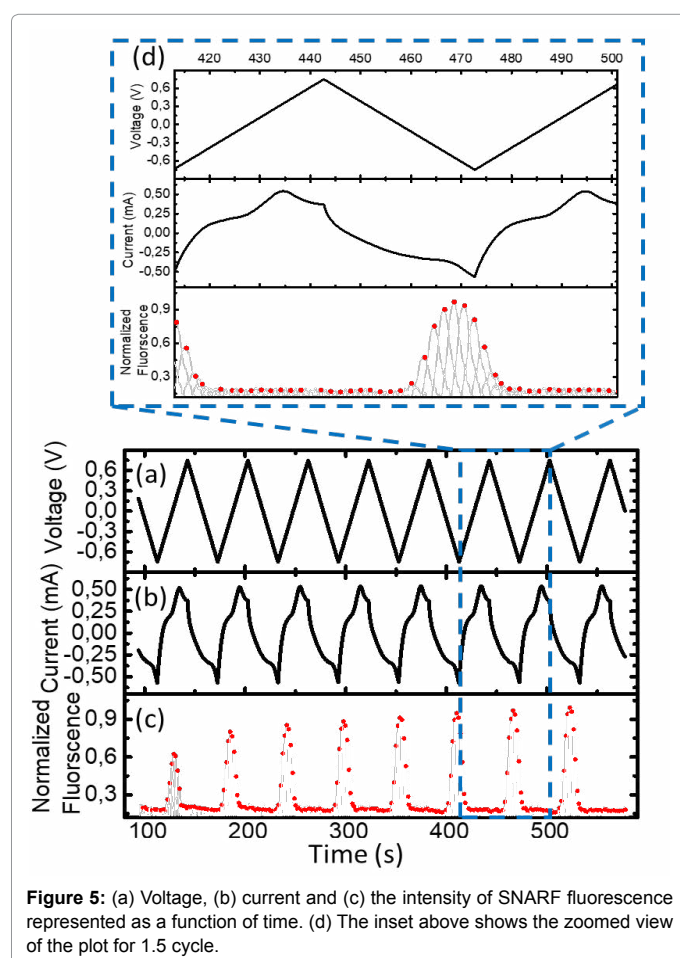


Figure 5: (a) Voltage, (b) current and (c) the intensity of SNARF fluorescence represented as a function of time. (d) The inset above shows the zoomed view of the plot for 1.5 cycle.

- pH change near a conducting polymer-coated electrode. *J electroanal Chem Interfacial Electrochem* 266: 297-308.
8. Lefebvre MC, Qi Z, Pickup PG (1999) Electronically Conducting Proton Exchange Polymers as Catalyst Supports for Proton Exchange Membrane Fuel Cells. Electrocatalysis of Oxygen Reduction, Hydrogen Oxidation, and Methanol Oxidation. *J Electrochem Soc* 146: 2054-2058.
 9. Maurer K, Cooper J, Caraballo M, Crye J, Suci D, et al. (2006) Electrochemically generated acid and its containment to 100 micron reaction areas for the production of DNA microarrays. *PLoS One* 1: e34.
 10. Frasconi M, Tel-Vered R, Elbaz J, Willner I (2010) Electrochemically Stimulated pH Changes: A Route To Control Chemical Reactivity. *J Am Chem Soc* 132: 2029-2036.
 11. Wang YC, Lin CB, Su JJ, Ru YM, Wu Q, et al. (2011) Electrochemically driven large amplitude pH cycling for Acid-Base driven DNA denaturation and renaturation. *Anal Chem* 83: 4930-4935.
 12. Cho SH, Kim D, Park SM (2008) Electrochemistry of conductive polymers. Effects of self-assembled monolayers of aminothiophenols on polyaniline films. *Electrochimica Acta* 53: 3820-3827.
 13. Ahao LB, Zhang M, Ren B, Tian ZQ, Wu DY (2014) Theoretical study on thermodynamic and spectroscopic properties of electro-oxidation of p-Aminothiophenol on Gold electrode surfaces. *J Phys Chem C* 118: 27113-27122.
 14. Zong S, Wang Z, Yang J, Cui Y (2011) Intracellular pH Sensing Using p-Aminothiophenol Functionalized Gold Nanorods with Low Cytotoxicity. *Anal Chem* 83: 4178-4183.
 15. Bishnoi SW, Rozell CJ, Levin CS, Gheith MK, Johnson BR, et al. (2006) All-Optical Nanoscale pH Meter. *Nano Lett* 6 (8): 1687-1692.
 16. www.klayout.de
 17. Johnson ID (2010) Molecular probes handbook. Life Technologies Corporation 11: Chapter 20.
 18. Balakrishnan D, Lamblin G, Thomann JS, Guillot J, Duday D, et al. (2017) Influence of polymerization on the reversibility of low-energy proton exchange reactions by Para-Aminothiophenol. *Sci Rep* 7: 15401.
 19. Cussler EL (1997) Diffusion: Mass transfer in fluid systems. Cambridge University press.
 20. Balakrishnan D, Lamblin G, Thomann JS, van den Berg A, Olthuis W, et al. (2018) Electrochemical control of pH in nano-litre volumes. *Nano Lett* 18: 2807-2815.